SEMARAK ILMU PUBLISHING

Journal of Advanced Research in Fluid Mechanics and Thermal Sciences

Journal homepage:
https://semarakilmu.com.my/journals/index.php/fluid_mechanics_thermal_sciences/index
ISSN: 2289-7879

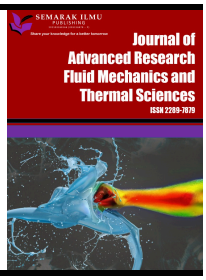

Dual Orifice Outlet Configurations in Backward Bent Duct Buoy (BBDB) for Enhanced Hydrodynamic Performance

Nurul Afiqah Mohd Azhar[1], Nurul Afiqah Mohd Azhar[1,*], Mohamad Alif Omar[2], Mohd Rosdzimin Abdul Rahman[3], Azfarizal Mukhtar[4], Mohd Kamarul Huda Samion[5], Yasutaka Imai[6], Mohd Rashdan Saad[7]

[1] Department of Mechanical Engineering, Faculty of Engineering, National Defence University of Malaysia (UPNM), Kuala Lumpur, Malaysia
[2] Institute of Sustainable Energy, Universiti Tenaga Nasional (UNITEN), Kajang, Malaysia
[3] Department of Mechanical Engineering. Centre for Defence Research & Technology (CODRAT), National Defence University of Malaysia (UPNM), Kuala Lumpur, Malaysia
[4] Department of Mechanical Engineering, Universiti Tenaga Nasional (UNITEN), Kajang, Malaysia
[5] Hydraulic and Instrumentation Laboratory, National Water Research Institute of Malaysia (NAHRIM), Seri Kembangan, Malaysia
[6] Institute of Ocean Energy, Saga University, Saga, Japan
[7] Department of Aeronautic Engineering & Aviation, Faculty of Engineering. Centre for Defence Research & Technology (CODRAT), National Defence University of Malaysia (UPNM), Kuala Lumpur, Malaysia

ARTICLE INFO

Article history:
Received 2 July 2025
Received in revised form 4 November 2025
Accepted 23 November 2025
Available online 17 December 2025

Keywords:
Renewable Energy, Ocean Energy, Wave Energy Converter (WEC), Oscillating Water Column (OWC), Backward Bent Duct Buoy (BBDB), Orifice

ABSTRACT

This research explored the Backward Bent Duct Buoy (BBDB), a type of Wave Energy Converter (WEC), to examine the relationship between the location of dual-orifice air column and the primary conversion efficiency. The BBDB type of WEC is promising due to its simple design and relatively strong performance, yet limited studies have investigated it, particularly concerning the orifice design, in comparison to other WEC types. The study aimed to investigate the impact of varying the location of the dual orifice air column of the BBDB device on its primary conversion efficiency. This was achieved by designing and fabricating three top panels each for horizontally and vertically aligned dual orifices with varying distance, tested in a 3D wave tank. The results indicated that the top panel with Configuration 2.3 exhibited the highest efficiency at 0.106%, followed by top panels with Configuration 1.3 (0.088%), Configuration 2.1 (0.085%), and Configuration 2.2 (0.082%). The findings suggest that top panels with vertically aligned dual orifices have higher efficiency compared to those with horizontally aligned dual orifices.

1. Introduction

Due to the increasing of population, technological advancement and economic progress, the demand for energy is escalating especially in emerging nations undergoing industrialization and urbanization. This however has led to arise in the utilization and depletion of fossil fuels on a global scale, reaching its zenith in 2016 as documented in a study by Dincer, Rosen and Khalid [1]. This

* *Corresponding author.*
E-mail address: nafiqah1003@gmail.com

https://doi.org/10.37934/arfmts.136.1.4657

pattern gives rise to a significant worry, particularly when considering the environment. The combustion of fossil fuels and the release of carbon dioxide contribute to substantial greenhouse emissions, posing harm to both humans and the environment [2]. The repercussions of a drop in energy supply can affect various aspects of society, the economy and the environment itself. Additionally, this trend aligns with sustainability concerns, given that fossil fuels are recognized as non-renewable energy sources with finite reserves. Consequently, there is a growing call for alternative energy sources that are sustainable and have minimal to no environmental impact, such as renewable energy.

Ocean energy refers to the diverse forms of renewable energy obtained from the ocean or sea. Given that about 70% of the Earth's surface is covered by oceans, these water bodies present a vast and potentially accessible reservoir of sustainable energy. Ocean energy is known for its high reliability, offering the prospect of continuous energy production, making it a promising solution for fulfilling power requirements. Notably, ocean energy surpasses other sources in reliability, with production occurring nearly 90% of the time, compared to 25% for both wind and solar devices. Ocean energy can be classified into three types: thermal energy, chemical energy, and mechanical energy. Examples of ocean energy sources include Ocean Thermal Energy Conversion (OTEC), tidal energy, and wave power [1][3][4]. OTEC harnesses the temperature difference between deep water and the ocean's surface, while tidal power utilizes the natural ebb and flow of tides to generate electricity, akin to a hydro-power plant. Lastly, wave power, also known as Wave Energy Converter (WEC), captures energy from wave motion and converts it into electricity. Ocean energy holds promise as a renewable energy source due to its constant availability and potentially lower environmental impact compared to some conventional energy sources. Nevertheless, the broader implementation of ocean energy technologies faces challenges, including technical, economic, and environmental considerations that require attention and resolution for successful adoption on a larger scale. Researchers believe that WEC has several advantages compared to other types of ocean energy. Researchers believe that WEC has several advantages compared to other types of ocean energy. Waves, being consistently in motion, offer the highest and most reliable energy density as it is a continual and replenishable energy source [5][6]. It also offers a more stable and predictable source of energy compared to other renewables energy like the wind. Offshore Wave Energy Converters (WECs) are commonly located away from the shores, mitigating their visual impact on coastal surroundings. This quality increases the likelihood of acceptance among communities that value the aesthetics of renewable energy installations.

Several types of Wave Energy Converters (WECs) exist, including the Oscillating Water Column (OWC), point absorbers, attenuators, and overtopping devices [7][8][9][10][11]. Among these, the OWC stands out for its simple body structure characterized by the absence of underwater moving components, ensures easy accessibility for maintenance, thereby extending its operational lifespan and making the power take-off unit easily accessible [12]. OWCs are categorized into two categories which are the fixed and floating type. Floating OWC systems come in four types: Forward Bent Duct Buoy, Backward Bend Duct Buoy (BBDB), Centre Buoy Pipe, and Sloped Buoy. The BBDB and Forward Bent Duct Buoy are cost-effective and feature a simple single floating structure. On the other hand, the Centre Buoy Pipe and Sloped Buoy utilize in-depth drafts, requiring special equipment for transportation and involving complex adjustments that extend installation time. Additionally, these latter types may incur higher mooring costs since the devices can withstand adverse weather conditions independently [13].

The BBDB is widely employed due to its shallow draft design, facilitating easy movement and installation. However, compared to other Wave Energy Converter (WEC) types, there is a limited body of research on the BBDB. According to Joubert, Niekerk, Reinecke and Meyer [14], only 3 out of the

172 listed WEC types are categorized as BBDB, specifically the Ocean Energy (OE) buoy or OE 35, OE Generation Platform or OE 12, and a developing 5kW floating offshore Oscillating Water Column (OWC) from the Guangzhou Institute of Energy Conversion (GIEC). It's noteworthy that both OE 35 and OE 12 are quarter-scale prototype models. The OE buoy is environmentally friendly, with no open moving parts that could harm marine life. Additionally, its turbines and generators are situated outside of the water, making maintenance easy, preventing corrosion, and ensuring accessibility [14].

Kim, Ko and Kim [15] has conducted a study regarding the shape geometry of a floating oscillating water columns which resulted in a rounded corner shape having a higher power output compared to sharp corner shapes and was supported by a study from Aiman et al. [16] where a higher primary efficiency was obtained at a low value of λ/L when using a rounded corner shape. As for the front shape of the BBDB device, a pentagonal front shape was proven to have a better efficiency [17][18][19][20].

Based on a study by Diaz, Sannasiraj and Soares [21], it is said that the wave height has a remarkable impact on the efficiency and so does the mooring characteristics. For both random and regular wave, the mooring that produce a smaller surge motion would further increase the efficiency of the device. A finding by Rezanejad, Soares, Lopez and Carballo [22] also verified that greater wave height led to increased device efficiency during extended wave periods. However, elevating the wave height would enhance device performance in conditions of low damping, irrespective of the wave period.

In a comparative study evaluating the performance of a single Oscillating Water Column (OWC) array and a Multi-OWC (M-OWC), Doyle and Aggidis [23] observed that the M-OWC generated higher flow rates and power in comparison to the single OWC device. However, when assessing efficiency and total capture width values, the WEC's efficiency relative to the total capture width decreased as the spacing between devices increased. Notably, existing M-OWC studies have not explored the utilization of multiple orifices for each individual OWC. Consequently, this research was conducted to address this gap and investigate the use of dual orifices in OWC systems.

Up until now, the predominant focus of existing studies has been on exploring the impact of factors such as corner geometry shape, front shape, duct extension, multi-OWC configurations and mooring characteristics on the performance of Backward Bent Duct Buoy (BBDB) devices. However, there is a noticeable dearth of studies examining the characteristics of the orifice, particularly with regard to how the location of dual orifices influences BBDB device performance. Recognizing that this knowledge gap can impede advancements in improving BBDB devices and their efficacy, this study aims to fill this void by investigating the effects of employing different location of dual orifices air column on BBDB device performance. The hypothesis posits that optimizing the orifice configuration will lead to enhanced BBDB performance.

2. Materials and Methods

2.1 Design and Fabrication of Top Panel Air Column

The design process for the location of the dual orifices for the air column of BBDB involves the utilization of SolidWorks CAD software. In Fig. 1, the drawing and dimensions of the BBDB device are illustrated from different perspectives. Meanwhile, Fig. 2 presents the design variations of the top panel, showcasing different configurations. The diameters for the orifice and other access holes were set at 40 mm, 10 mm and 20 mm respectively.

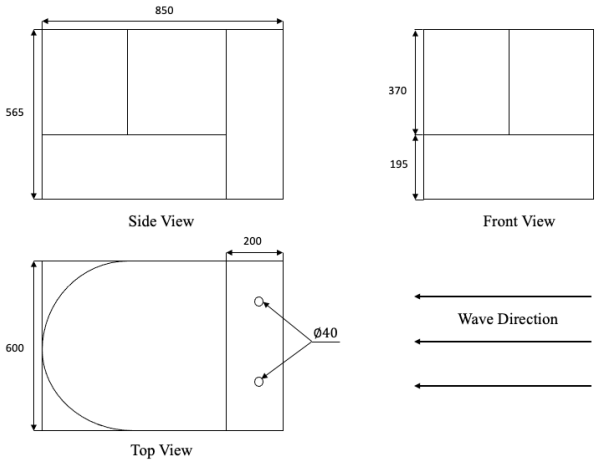

Fig. 1. Drawing of BBDB from 3 different perspective

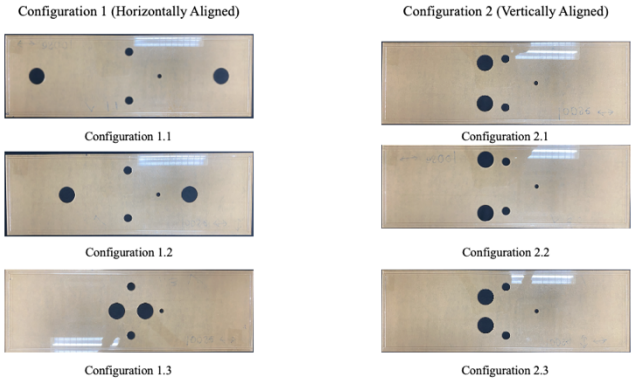

Fig. 2. Fabricated Top Panels

The overall dimensions of BBDB device were adopted from a previous study by Aiman et al. [16], along with the measurements for the orifice diameter [16][24][25]. Prior to conducting the wave tank test, the top panels of the air columns were fabricated using acrylic sheet materials and a laser cutting method, as depicted in Fig. 2.

2.2 3D Wave Basin Test

A 3D wave basin facility within Hydraulic and Instrumentation Laboratory, National Water Research Institute of Malaysia (NAHRIM) was used to conduct the experiment. The same facility was also used for few other studies conducted in the past [16][26]. The dimensions of the 3D wave basin are 30 m length, 30 m width, 1.2 m in depth and water depth of 0.04 m. Top view of BBDB setup is as shown in Fig. 3. In order to replicate low heave wave conditions, the study employed a combination of 0.10 m wave height and 1 s to 3 s wave periods. The wavelength for this experiment ranges from 0.61 to 1.843 which makes it a shallow water condition.

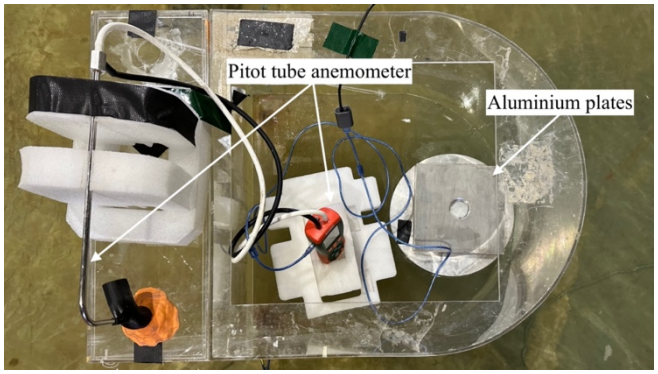

Fig. 3. Device setup from top view

2.3 Instrumentation

A pitot tube anemometer EXTECH HD_350 ((0.0001 m^3/min accuracy) was attached on top of the top panel to measure the pressure and the flow rate output from the orifice. A wave probe was placed 3 m upstream from the device to measure the height of the incoming wave. This measure was implemented to guarantee uniformity between the output of wave height and the input of wave height. Two mooring lines, each equipped with concrete blocks on their opposite ends, were affixed to both sides of the model's bottom. This arrangement aimed to prevent any displacement of the Backward Bent Duct Buoy (BBDB) during the experiment. Additionally, an extra weight of 10.5 kg was inserted inside the front buoy of the BBDB to ensure its stability post-deployment.

The operation of the 3D wave basin and wavemaker was centrally managed from a control room. Prior to initiating the wave test, specific parameters including wave height and period were predetermined. Subsequently, the wave paddle oscillated to generate waves within the wave basin. It's noteworthy that a uniform wave height of 0.1 m was employed for conducting the experiment across all top panels, as it yielded the most optimal output.

2.4 Primary Performance of Oscillating Water Column

In this study, the primary conversion efficiency of the BBDB device was computed (1), which was derived from Macfarlane et al. [27]. Calculating the BBDB efficiency necessitated the determination of both wave energy and air energy. Therefore, it was imperative to quantify the wave energy and air energy generated throughout the course of the experiment.

$$n_1 = \frac{E_{air}}{E_{wave}} \tag{1}$$

Wave energy, denoting the energy acquired from incident waves, was computed in this study using (2).

$$E_{wave} = \frac{1}{2}\rho g \zeta^2 C_g B \tag{2}$$

In the given equation, where g, ρ, B, ζ, C_g, Ω, k, λ and h are the gravitational accelerations (m/s^2), water density (kg/m^3), width of the OWC device perpendicular to the incident wave direction, incident wave amplitude (m), the group velocity (m/s), angular frequency of the wave(rad/s), wave number, wavelength (m) and water depth (m) respectively. The Group Velocity, C_g signifies the speed with which a wave packet travels, and its equation is defines in (3).

$$C_g = \frac{\Omega}{2k}\left(1 + \frac{2kh}{sinh(2kh)}\right) \quad (3)$$

Meanwhile, wave number. k represents the spatial frequency of a wave, measured in cycles per unit distance (ordinary wavenumber) or radians per unit distance (angular wavenumber) as shown in (4). Here, λ denotes the angular frequency of the wave (rad/s).

$$k = \frac{2\pi}{\lambda} \quad (4)$$

Conversely, air energy in this study pertains to the pneumatic output energy derived from the orifice situated at the top panel column. The calculation of air energy in the study utilized (5); however, it was imperative to ascertain the pressure difference output for accurate computation.

$$E_{air} = \frac{1}{T}\Delta P(t)Q(t)dt \quad (5)$$

In this context, the pressure difference, ΔP, was established by subtracting the maximum and minimum pressure obtained while Q represented the flow rate acquired from inside of the water column. Additionally, the calculation for E_{air} of the top panel with 1 orifice is shown in (5). However, since this study involves using dual orifices, the E_{air} of each orifice with the same wave height and period were initially summed up before divided with E_{wave} as shown in (6).

$$\Sigma E_{air} = E_{air1} + E_{air2} + \cdots + E_{airn} \quad (6)$$

3. Results and Discussion

3.1 Pressure in Water Column

Pressure is a crucial factor in determining the efficiency of the BBDB device. As per the air energy formula in (5), the pressure difference significantly impacts the air energy, subsequently affecting the overall efficiency. Consequently, a higher pressure difference is advantageous, as it leads to an improvement in the device's efficiency.

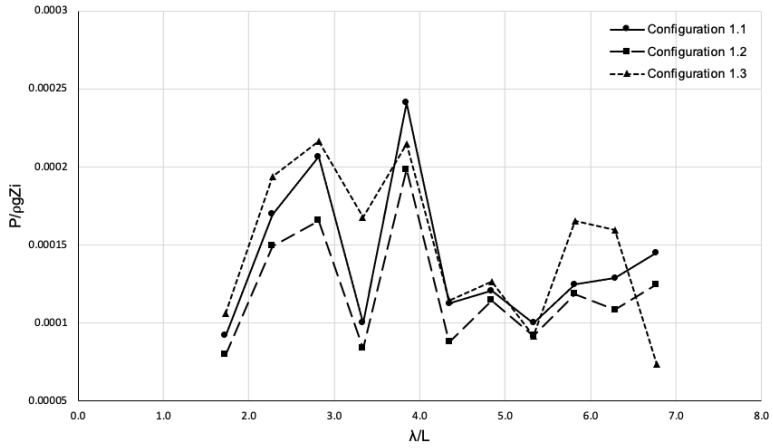

Fig. 4. Pressure Amplitude for Configuration 1

Based on Fig. 4, all three configurations have varying values. Nevertheless, the trajectories and underlying trends are similar. The trendline for all 3 top panels increases at λ/L=2.8 before declining

at λ/L=3.3, although configuration 1.3 sustained a significant value. All three configurations then spike significantly at λ/L=3.8 with configuration 1.1 reaching the highest value, 0.00024, compared to the other two. However, all three top panels dip close to the lowest points of trend. From λ/L=4.3 onwards, the configs values fluctuate up and down minimally. Configuration 1.3 however, increases rapidly at λ/L=5.8 before reduces to all time low value of 0.000075.

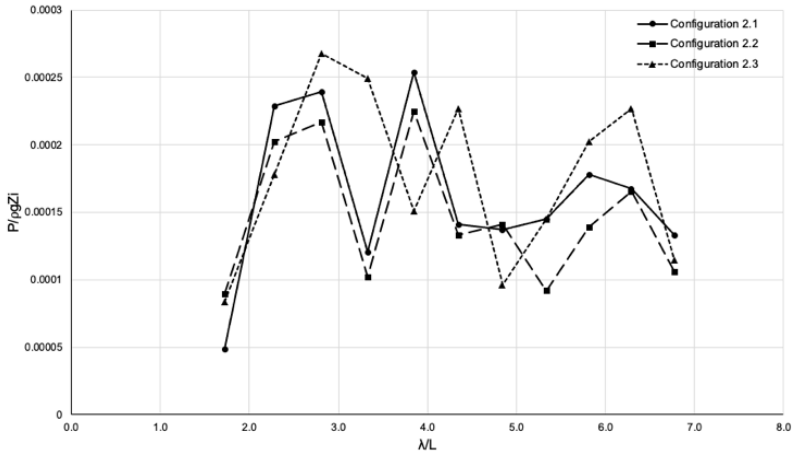

Fig. 5. Pressure Amplitude for Configuration 2

In the observed graph (Fig. 5), all three configurations exhibit a shared trend during the initial points at λ/L=1.7 to 2.8. At this stage, there is a noticeable and simultaneous drastic increase in values across all configurations. However, at λ/L=2.8, a distinctive shift occurs as the values sharply drop. This decline is followed by a subsequent increase, resulting in a secondary peak. Interestingly, the three configurations exhibit a pattern of stalling or minimal fluctuation after reaching this secondary peak except for configuration 2.3 where it reaches the third peak. Configuration 2.3 experienced the highest pressure amplitude of 0.00026 during its first peak.

3.2 Flow Rate at the Orifice Outlet

The flow rate is a key factor in determining the kinetic energy of the moving air within an oscillating water column (OWC) system. In the context of energy conversion in an OWC, this kinetic energy is a critical component. Therefore, a higher flow rate generally results in increased kinetic energy, which, in turn, contributes to more efficient energy conversion within the OWC system.

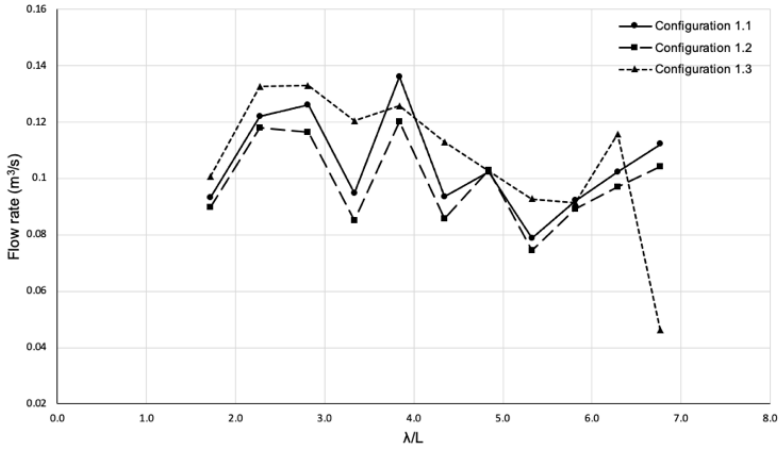

Fig. 6. Air flow rate at the orifice outlet in Configuration 1

From λ/L 1.7 to 3.8, all three configurations have parallel trends at different values. Whereas at λ/L=3.8 onwards, configuration 1.1 and 1.2 have similar fluctuating trajectory but configuration 1.3 continues the trend with relatively small fluctuation consistently. With configuration 1.3 having the upper value, the flow rates of all 3 configurations increases as λ/L increases from 1.7 to 2.8. Then as the λ/L increases to 3.3, the flowrates decrease steeply except for 1.3. At λ/L=3.8, flowrates of configuration 1.1 and 1.2 spike to their peaks of 0.13 and 0.12 respectively. Configuration 1.3 however experiences a slight increase of flowrate. Beyond λ/L=3.8, the flowrates fluctuate similarly to the pressure amplitude trends.

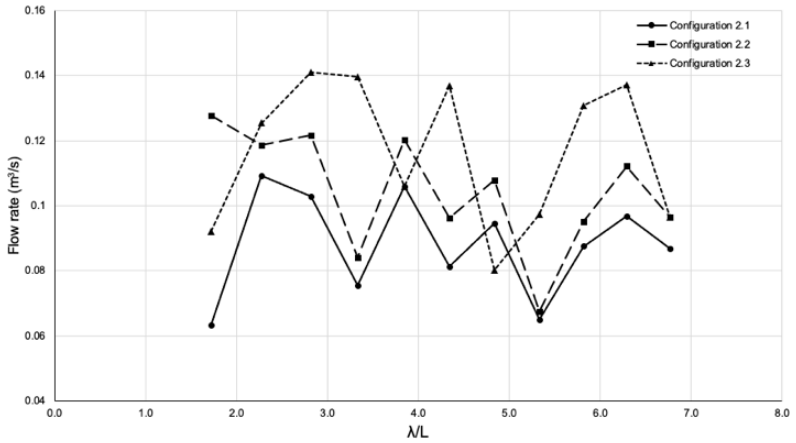

Fig. 7. Air flow rate at the orifice outlet in Configuration 2

Fig. 7 illustrates dynamic variations in flow rates among the configurations across different periods of λ/L. Notably, configuration 2.1 and 2.2 exhibit a similar trend from low period to high period of λ/L with varying values. However, configuration 2.2 has a higher value compared to configuration 2.1. In contrast, configuration 2.3 deviates from this trend, showcasing a distinctly different pattern. Configuration 2.3 attains the highest flow rate of 0.14 during λ/L=2.8 and maintains significantly high flow rates at λ/L=2.8 to 3.3 and λ/L=5.8 to 6.3. During the lowest λ/L, configuration 2.2 stands out with the highest flow rate, reaching 0.127 before experiencing a subsequent decline.

3.3 Primary Conversion Efficiency

The primary conversion efficiency was calculated and plotted according to (1)[27]. The primary conversion efficiency for Configuration 1 (horizontally aligned) with a wave height of 0.1 m is as shown in Fig. 8. Based on the graph shown, it can be seen that both configurations 1.2 and 1.3 have a slightly similar trend which increasing moderately from λ/L = 1.7 to 2.3. and reaches the peak at λ/L =2.3. However, after reaching the peak, it started decreasing rapidly until λ/L = 3.3 where the efficiency is less than half of its peak efficiency. Whereas for configuration 1.1, it reaches the peak at λ/L=2.8 before stalling at λ/L=3.3 and increase rapidly again at λ/L=3.8. Configuration 1.3 has the highest peak efficiency of 0.088%, followed by configuration 1.1 with efficiency of 0.073% and configuration 1.2 being the lowest. The efficiency for all configuration 1 is higher during the low periods of λ/L.

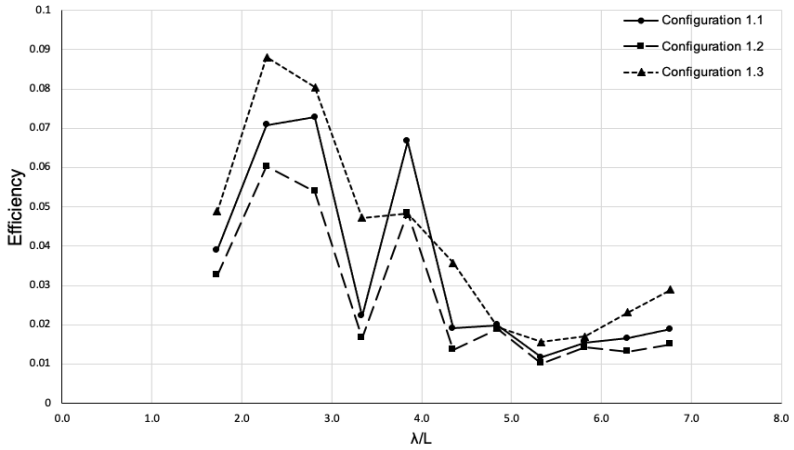

Fig. 8. Efficiency of device for Configuration 1

As for Configuration 2 (vertically aligned), configuration 2.3 emerges with the highest efficiency of 0.106%, surpassing the others by 22% difference as can be seen in Fig. 9. In contrast, the difference between configuration 2.1 and 2.2 is minimal, standing at 3.6%. Based on the graph plotted, it can be seen that configurations 2.1 and 2.3 share the same trendline where there's a rapid increase in efficiency, followed by a steep decline before a subsequent increase. Compared to configuration 2.2, where the efficiency increases gradually at λ/L=1.7 to 2.3 and started decreasing afterwards. However, both configuration 2.1 and 2.2 reaches their efficiency peak at λ/L=2.3 whereas the peak efficiency for configuration 2.3 is at λ/L=2.8. At λ/L= 3.3 to 4.8, the efficiency for all three top panels exhibits fluctuations before settling into a more consistent trendline.

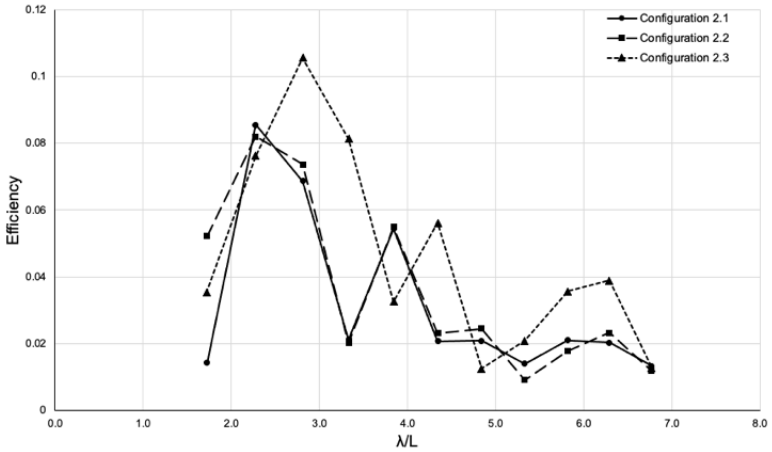

Fig. 9. Efficiency of device for Configuration 2

Fig. 10 illustrates the efficiency trends for both Configuration 1 and Configuration 2. Notably, Configuration 2.3 stands out with the highest efficiency, reaching a peak of 0.11%, surpassing other top panels. Following closely are Configuration 1.3, Configuration 2.1, and Configuration 2.2, peaking at 0.088%, 0.085%, and 0.082%, respectively. A notable rapid increase in efficiency occurs between λ/L = 1.7 and 2.8, followed by a steep decrease and a subsequent rise at λ/L = 3.8. Configurations 1.2, 1.3, 2.1, and 2.2 share a similar trendline, reaching their peaks at λ/L = 2.3 before a decline until λ/L=3.3. Configuration 1.2 exhibits the lowest peak efficiency at 0.06%, marking a 55.4% difference from Configuration 2.3.

Overall, the data indicates that the efficiency is higher during the low period of λ/L, and as this period increases, efficiency decreases. Beyond λ/L=4.3, there are no significant changes observed.

The relatively low percentage of primary conversion efficiency is attributed to the shallow water conditions outlined in the Materials and Methods sections. In shallow water, the interaction between waves and the seabed becomes more pronounced, potentially impacting the efficiency of wave energy. Additionally, it imposes limitations on the submergence depth of the device, a critical factor determining the air column's volume.

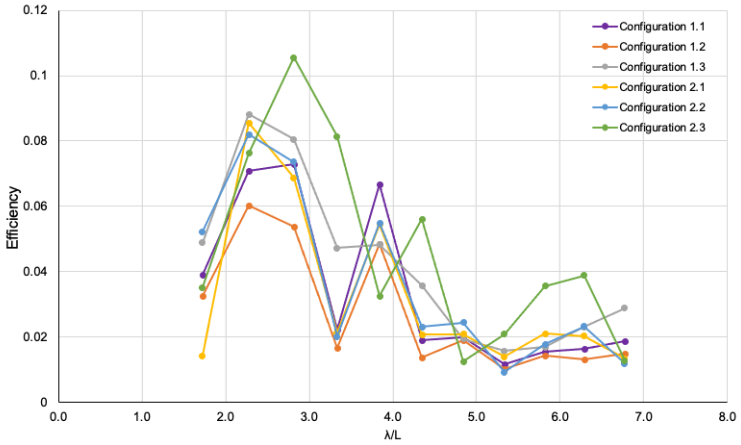

Fig. 10. Overall Efficiency of BBDB device

4. Conclusion

The results reveal that Configuration 1.3 exhibits the highest efficiency at 0.088%, surpassing other top panels. The percentage difference in efficiency between Configuration 1.3 and 1.1 is 18.6%, while it is 37.8% when compared to Configuration 1.2.

In the case of Configuration 2, Configuration 2.3 stands out with the highest efficiency at 0.11%. This configuration demonstrates a 25.6% and 29.2% percentage difference in efficiency when compared to Configuration 2.1 and Configuration 2.2, respectively.

Notably, Configuration 2.3 attains the highest overall primary conversion efficiency of 0.11%, outperforming other top panels. Collectively, the data strongly supports the conclusion that Configuration 2 surpasses Configuration 1 in terms of efficiency.

However, it is important to note that the data in this study were restricted to primary conversion efficiency. Additionally, as the study was conducted in shallow water conditions, the generated wave conditions may not precisely represent the complexities of actual ocean waves. This limitation highlights an opportunity for future research to enhance the study scope by incorporating data for secondary conversion efficiency. Conducting similar experiments in a 3D wave basin that replicates real-world wave conditions could provide more comprehensive insights.

The findings of this study, while constrained by these limitations, can still be valuable as a reference for researchers exploring the validation of simulation results. Furthermore, the applicability of our results can be extended to other research endeavors that utilize a Backward Bent Duct Buoy (BBDB) configuration.

Acknowledgement

This research received support from Joint Research/Usage for Institute of Ocean Energy Saga University Japan 2023 (Acceptance No: 23B09). The authors would also like to extend their gratitude to Universiti Pertahanan Nasional Malaysia (UPNM) for sponsoring the project through the Graduate Research Assistant Fellowship under the PPPI Trust Fund UPNM.

References

[1] Dincer, I., M. A. Rosen, and F. Khalid. "Ocean (Marine) Energy Production." *Comprehensive Energy Systems* 3 (2018). https://doi.org/10.1016/b978-0-12-809597-3.00316-3

[2] Wuebbles, Donald J., and Atul K. Jain. "Concerns about climate change and the role of fossil fuel use." *Fuel processing technology* 71, no. 1-3 (2001): 99-119. https://doi.org/10.1016/s0140-6701(02)80664-6

[3] Fusheng, Li, Li Ruisheng, and Zhou Fengquan. "Microgrid technology and engineering application." *China Electric Power Press: Elsevier Inc* (2016). https://doi.org/10.1016/c2013-0-18521-2

[4] Aderinto, Tunde, and Hua Li. "Ocean wave energy converters: Status and challenges." *Energies* 11, no. 5 (2018): 1250. https://doi.org/10.3390/en11051250

[5] Drew, Benjamin, Andrew R. Plummer, and M. Necip Sahinkaya. "A review of wave energy converter technology." (2009): 887-902.

[6] Zhang, D., Li, W., & Lin, Y. "Wave energy in China: Current status and perspectives." *Renewable Energy* (2009). https://doi.org/10.1016/j.renene.2009.03.014

[7] Dolores, E. M., Jose, S. L., & Vicente, N. "Classification of Wave Energy Converters." *Recent Adv Petrochem Science* (2017). https://doi.org/10.19080/rapsci.2017.02.555593

[8] Falcao, Antonio F. de O. "Wave energy utilization: A review of the technologies." *Renewable and sustainable energy reviews* 14, no. 3 (2010): 899-918. https://doi.org/10.1016/j.rser.2009.11.003

[9] Lindroth, Simon, and Mats Leijon. "Offshore wave power measurements—A review." *Renewable and Sustainable Energy Reviews* 15, no. 9 (2011): 4274-4285. https://doi.org/10.1016/j.rser.2011.07.123

[10] Astariz, Sharay, and Gregório Iglesias. "The economics of wave energy: A review." *Renewable and Sustainable Energy Reviews* 45 (2015): 397-408. https://doi.org/10.1016/j.rser.2015.01.061

[11] Pietra, L., M. Tello, J. Bhattacharjee, and C. Guedes Soares. "Review and classification of wave energy converters." *Centre for Marine Technology and Engineering (CENTEC), Instituto Superior Técnico, Lisboa, Portugal. doi* 10 (2012). https://doi.org/10.1201/b12726-84

[12] Wu, Bijun, Tianxiang Chen, Jiaqiang Jiang, Gang Li, Yunqiu Zhang, and Yin Ye. "Economic assessment of wave power boat based on the performance of "Mighty Whale" and BBDB." *Renewable and Sustainable Energy Reviews* 81 (2018): 946-953. https://doi.org/10.1016/j.rser.2017.08.051

[13] Murakami, Tengen, Yasutaka Imai, Shuichi Nagata, Manabu Takao, and Toshiaki Setoguchi. "Experimental research on primary and secondary conversion efficiencies in an oscillating water column-type wave energy converter." *Sustainability* 8, no. 8 (2016): 756. https://doi.org/10.3390/su8080756

[14] Joubert, J. R., Niekerk, J. L. V., Reinecke, J., & Meyer, I. "Wave Energy Converters (WECs)." Centre for Renewable and Sustainable Energy Studies, 2013.

[15] Kim, Sung-Jae, Weoncheol Koo, and Moo-Hyun Kim. "Nonlinear time-domain NWT simulations for two types of a backward bent duct buoy (BBDB) compared with 2D wave-tank experiments." *Ocean engineering* 108 (2015): 584-593. https://doi.org/10.1016/j.oceaneng.2015.08.038

[16] Aiman, Muhamad Jalani, Nur Izzati Ismail, Mohd Rashdan Saad, Yasutaka Imai, Shuichi Nagata, Mohd Kamarul Huda Samion, Ernie Abd Manan, and Mohd Rosdzimin Abdul Rahman. "Study on shape geometry of floating oscillating water column wave energy converter for low heave wave condition." *Journal of Advanced Research in Fluid Mechanics and Thermal Sciences* 70, no. 2 (2020): 124-134. https://doi.org/10.37934/arfmts.70.2.124134

[17] Wu, Bi-jun, Meng Li, Ru-kang Wu, Yun-qiu Zhang, and Wen Peng. "Experimental study on primary efficiency of a new pentagonal backward bent duct buoy and assessment of prototypes." *Renewable energy* 113 (2017): 774-783. https://doi.org/10.1016/j.renene.2017.06.010

[18] Li, Meng, Ru-kang Wu, Bi-jun Wu, and Yun-qiu Zhang. "Experimental study on conversion efficiency of a floating OWC pentagonal backward bent duct buoy wave energy converter." *China Ocean Engineering* 33 (2019): 297-308. https://doi.org/10.1007/s13344-019-0029-1

[19] Wu, Bijun, Meng Li, Rukang Wu, Tianxiang Chen, Yunqiu Zhang, and Yin Ye. "BBDB wave energy conversion technology and perspective in China." *Ocean Engineering* 169 (2018): 281-291. https://doi.org/10.1016/j.oceaneng.2018.09.037

[20] Li, Meng, Bi-jun Wu, Chuan-you Jiang, and Yun-qiu Zhang. "Effect of reciprocating and unidirectional airflow on primary conversion of a pentagonal Backward Bent Duct Buoy." *Applied Ocean Research* 89 (2019): 85-95. https://doi.org/10.1016/j.apor.2019.05.010

[21] Díaz, H., S. A. Sannasiraj, and C. Guedes Soares. "Experimental study of behaviour and efficiency on a backward bent duct buoy." In *Advances in Renewable Energies Offshore: Proceedings of the 3rd International Conference on Renewable Energies Offshore (RENEW 2018), October 8-10, 2018, Lisbon, Portugal*, p. 409. CRC Press, 2018.

[22] Rezanejad, K., C. Guedes Soares, I. López, and R. Carballo. "Experimental and numerical investigation of the hydrodynamic performance of an oscillating water column wave energy converter." *Renewable Energy* 106 (2017): 1-16. https://doi.org/10.1016/j.renene.2017.01.003

[23] Doyle, Simeon, and George A. Aggidis. "Development of multi-oscillating water columns as wave energy converters." *Renewable and sustainable energy reviews* 107 (2019): 75-86. https://doi.org/10.1016/j.rser.2019.02.021

[24] Imai, Yasutaka, Kazutaka Toyota, Shuichi Nagata, Toshiaki Setoguchi, Junko Oda, Narimasa Matsunaga, and Takafumi Shimozono. "An Experimental Study of Negative Drift Force Acting on a Floating OWC "Backward Bent Duct Buoy"." In *International Conference on Offshore Mechanics and Arctic Engineering*, vol. 48203, pp. 871-879. 2008.

[25] Imai, Yasutaka, Kazutaka Toyota, Shuichi Nagata, and Mohammad AH Mamun. "Duct extension effect on the primary conversion of a wave energy converter 'backward bent duct buoy'." *J. OTEC* 15 (2010): 33-35.

[26] Husain, MK Abu, NI Mohd Zaki, SM Che Husin, N. A. Mukhlas, S. Z. A. S. Ahmad, N. Abu Husain, and AH Mohamed Rashidi. "Integrated tidal marine turbine for power generation with coastal erosion breakwater." *Int. J. Civ. Eng. Technol* 10, no. 2 (2019): 1277-1293.

[27] Elhanafi, Ahmed, Gregor Macfarlane, Alan Fleming, and Zhi Leong. "Experimental and numerical investigations on the hydrodynamic performance of a floating–moored oscillating water column wave energy converter." *Applied energy* 205 (2017): 369-390. https://doi.org/10.1016/j.apenergy.2017.07.138